EFFECT OF DEBONDING MICROPROCESSES ON PARTICULATE FILLED POLYOLEFINES FLOW AND FRACTURE. I. YIELD STRESS[1]

Victor G. Oshmyan, Irena L. Dubnikova

N.N.Semenov Institute of Chemical Physics Russian Academy of Sciences,
Kosygin st. 4, 117977 Moscow

SUMMARY: Effect of filler fraction and size on debonding mechanism, debonding stress, portion of debonded particles and yielding of particulate filled polypropylene (PP) and polyethylene (HDPE) have been studied. Transitions from uncorrelated to correlated debonding and (as a consequence) from microuniform to craze-like flow at approximately $\Phi = \Phi_c \approx 15$ vol.% of filler fraction have been discovered. The transition between debonding mechanisms is caused by an increase in the intensity of mechanical fields interaction with loading. The phenomenon has been described in terms minimum work criterion. Theoretical estimation of the transitional loading as 11 vol.% is slightly below the experimental value.

KEYWORDS: polymer, filler, composites, mechanical properties, yielding, debonding

INTRODUCTION

Effect of debonding in particulate filled composites on macroscopic properties is mainly simulated by the way of modeling of the initial portions of stress-strain curves under the limiting assumptions of complete debonding or perfect bond between components [1]. In particular, the dependencies of the initial slop (Young modulus, E) and peak height (yield stress, σ_y) upon filler volume fraction, Φ, are calculated. Mostly the role of scaling factor of inclusion size d (the scaling factor) is neglected. Nicolais and Narkis [2] proposed the model of the minimally loaded effective cross-section

$$\sigma_{y(d)}^{rel} = \frac{\sigma_{y(d)}}{\sigma_y^m} = 1 - \alpha\Phi^{2/3} \qquad (1)$$

[1]The work is supported by Russian Foundation of Fundamental Research, grant No. 97-03-32808.

for the case of complete debonding. Subscript (*d*) points to complete debonding as well as subscript (*b*) will point to the case of perfect bond. Superscript *rel* is referred to the ratio of composite value to that of matrix. Naturally, (1) predicts decreasing concentration dependence. Composite yield stress was computed in [3] by the way of numerical solution of continuum mechanics boundary problems both for the cases complete debonding and perfect bond in frameworks of periodic structural model. the results obtained are very close to that of [2] in the debonding case. However, an increase in yield stress with F was found for strong interfacial interaction.

The majority of experimental data [4,5] coincides with the results of simulations obtained assuming low adhesion. At the same time, in a number of works devoted to the role of hard particle size other tends were revealed. In particular, Vollenberg and co-authors [6-7] observed a drastic increase in *E* when using nanoparticles in PS, PC, and PP-based composites. The transition to the ascending concentration dependence $\sigma_y(\Phi)$ was disclosed for the PP and LDPE-based composites with ultrafine particles [9-11]. The explanations reported by authors for the effects observed are ambiguous. There are approaches explaining the effect of *d* on the composite deformation parameters by the dependence of polymer morphology on the particle diameter due to their nucleating action [6]. Similar hypothesis is based on the idea that the interphase of special morphology is formed [7, 8, 12, 13]. It is supposed to be of the independent of *d* thickness. Thereby a decrease in particle size at fixed Φ should result in an increase in the interphase fraction and in variation of the properties by the way. It was assumed [9] that the reason for the dependence of *E* and σ_y on filler dispersity may be related to the enhanced ability of the small inclusions to agglomerate, and hence, to the formation of hard clusters. Voros and Pukanszky [11] estimated σ_y assuming that the inclusions carry a fraction of loading proportional to the interfacial debonding stress σ_d, which in turn increases with a decrease in *d* [14,15]. The mechanism of stress redistribution accepted in [11] has not been sufficiently substantiated because the effect of σ_d on the fraction of debonded inclusions is not analyzed.

It was shown by X-ray diffraction and DSC techniques that the crystalline structure of PP and HDPE matrices not substantially changed upon the addition of a filler up to 50 vol.% ($Al(OH)_3$ and glass spheres of the diameter range from 0.2 to 55 μm). At the same time it was established that macroscopically deformational behavior of filled high plastic polymers with nonideal adhesion is essentially attributed to micropores formation caused by debonding [16-18]. Filler fraction and size were demonstrated to be the main factors, which determine the regular trends in the interfacial failure [14,15, 18-22].

In this work the theory is developed to explain the effect of particle size on the yield stress of filled polymers under the influence of the debonding stress on the fraction of debonded particles within the framework of various mechanisms of interfacial failure. The effect of inclusions content and size on the yield stress of PP and HDPE- based composites is also studied experimentally.

EXPERIMENTAL

Isotactic PP with $\overline{M}_w = 63\times10^5$, $\overline{M}_w/\overline{M}_n = 35$ and HDPE with $\overline{M}_w = 14\times10^5$, $\overline{M}_w/\overline{M}_n = 8$ (gel permeation chromatography) were used as the polymeric matrices. Narrow fractions of $Al(OH)_3$ (Sumitomo Smelting Co., Japan) and glass spheres were employed as the fillers. The particle mean diameters were of 0.2, 3.5 μm (glass spheres) and of 1, 2.5, 8, 25, 55 μm ($Al(OH)_3$).

PP-based composites were prepared by melt mixing on a twin-screw mixer in presence of calcium stearate (2% of the filler weight) and the stabilizers against thermal oxidation. Mixing temperature was 190°C, the screw rate was 40 rpm and the mixing time was 10 min. HDPE-based composites were prepared by both blending (at 175°C) and polymerization [19] methods.

Testing specimens (0.5-mm-thick plates) were prepared by pressing at 10 MPa and 190°C (PP) and 175°C (HDPE). The specimens were cooled under pressure at a rate of 20 K/min. Specimens were tested on Instron- 1122 machine at a relative deformation rate of 0.67 min^{-1} and at room temperature.

The microprocesses of deformation and the surface microstructure of the deformed specimens were studied with a JSM-35 scanning electron microscope.

RESULTS AND DISCUSSION

Uncorrelated and Correlated Debonding Mechanisms

Single debonding locally alters the stress and strain distribution, which may be important for debonding on different inclusion. The effect is negligible at small Φ. As a result the debonding proceeds in an uncorrelated manner (Fig. 1a). As the distance between particles decreases with Φ interaction between mechanical fields of neighboring particles becomes noticeable. Because of the maximum stress concentration at the pore equator one should expect consistent particle debonding in the transverse direction with respect to loading (Fig. 1b).

The occurrence of two interfacial failure mechanisms was disclosed experimentally by in situ tensile testing of the PP-$Al(OH)_3$ composite specimens in the electron microscope chamber [20,21]. The transition from uncorrelated to correlated debonding takes place at $\Phi \approx 15$ vol.%.

Critical filler fraction was calculated in [22,23]. The model of debonding accumulation in the course of loading was developed, allowing to describe the stress-strain curves in the region of elastic deformation within the framework of the uncorrelated and correlated debonding mechanism. This model is based on the balance between the tensile work, stored elastic energy and energy spent for the formation of new surfaces. The criterion for the implementation of the first or second mechanism in a model is the smallest value of tensile work or (as equivalent) the deformation ε_d at which the debonding process begin. As evidenced by the analysis of the concentration dependence of the deformation ratio $\varepsilon_d^u/\varepsilon_d^c$ corresponding to uncorrelated and correlated debondings, respectively, the first mechanism is preferable below critical filler fraction, Φ_c, while the second becomes energetically more advantageous above Φ_c. Transitional filler fraction value rises with the

broadening the particle size distribution, however, it quickly reaches saturation point corresponding to about 11 vol.%.

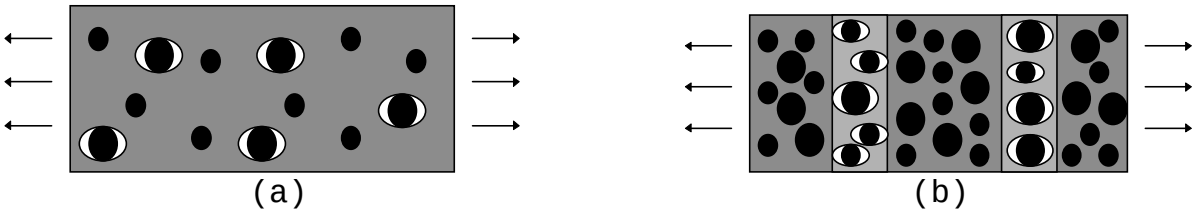

Fig. 1: Scheme of uncorrelated (a) and correlated (b) debonding mechanisms.

Microuniform and Craze-like Mechanisms of Pore Plastic Growth

Low filler fraction (below Φ_c) causes low micropores volume content. As a result, localized pattern of the plastic flow, which is typical for the matrices employed, is retained. The pore initiate the polymer local flow: When the pore concentration increases, the number of shear bands also increases. This effect is visually observed. Formation of a broad shear band, which further transforms into the neck region, corresponds to macroscopic yield stress load. Inside the neck region, the micropores are distributed in a diffuse manner. Their degree of stretching corresponds to the average degree of stretching in the neck region. This is an argument to characterize corresponding flow mechanism as "microuniform", nevertheless deformation be macroscopically nonuniform.

At Φ above Φ_c, inclusion correlated debonding occurs, and the deformation is mainly concentrated in the matrix ligaments between the formed pores. Hence, the plastic flow is for the most part localized in the deformation zones of the craze-like structure consisting of micropores and fibrillized polymer strands. For this region of Φ, the nonuniform pattern of material local deformation is typical, which is expressed by the alternating plastic and elastic deformation regions. The relevant flow mechanism may be characterized as "craze-like". The concentration of craze-like zones formed is responsible for the character of macroscopic deformation. If a large number of microporous zones is formed by the onset of macroscopic flow, the force-elongation curve is monotonous (or at least almost monotonous) and the sample is deformed by the uniform macroscopic mechanism. At low concentration of craze-like zones, the force-elongation curve is of extreme type and the flow in the bulk sample is localized within the narrow region with an increased concentration of microporous zones.

The Effect of Inclusion Size on the Composite Yield Stress

Figure 2 shows the experimental data for the relative yield stress, σ_y^{rel}, of the filled PP and HDPE. Calculated concentration dependencies [3] are depicted by solid lines. Periodical structural model for the composites was accepted and limiting assumptions with respect to interfacial bond were made: complete debonding, $\sigma_{y(d)}^{rel}(\Phi)$, (curve 1) and perfect bond, $\sigma_{y(b)}^{rel}(\Phi)$, (curve 2). Curve 1 agrees well with the dependence (1) predicted by the model of the minimum effective loaded cross-section [2].

It is seen that the experimental data are described by the $\sigma_{y(d)}^{rel}(\Phi)$ function up to a certain degree of filling, Φ_d. Above this value σ_y drops more slowly when compared to $\sigma_{y(d)}(\Phi)$. This circumstance seems to be a convincible argument to consider $\sigma_{y(d)}^{rel}(\Phi)$ as a basic yield stress concentration dependence. The more is d, the more is Φ_d. Particularly, the deflection is not observed in the entire range studied (Φ_d > 50%) when $d \geq 25$ μm in the case of PP matrix. Another regular trend is the higher Φ_d value for the higher matrix yield stress (σ_y^{PP} = 35 MPa > σ_y^{HDPE} = 25 MPa). For example, $\Phi_d \approx 15\%$ and $\approx 5\%$ at d = 1 μm for PP- and HDPE-based composites correspondingly.

It was shown [14,15] that the debonding takes place within the specific stress interval, $\sigma_{d,min} \leq \sigma_d \leq \sigma_{d,max}$, which is slightly dependent on Φ. As d increases, the range of debonding stresses shifts to lower values. The effect of σ_d on the portion, x_d, of particles debonded by the onset of macroscopic flow is seen by us as the main reason for the effect of inclusion size on the yield stress of particulate filled polyolefines. Depending on the ratio between the range of debonding stress and the range possible yield stress values, $\sigma_{y(d)} \leq \sigma_y \leq \sigma_{y(b)}$, various conditions may be implemented. Namely, (i) all inclusions are debonded

$$x_d = 1, \tag{2}$$

the phase bond is completely retained

$$x_d = 0, \tag{3}$$

or interfacial processes are occurred but not completed

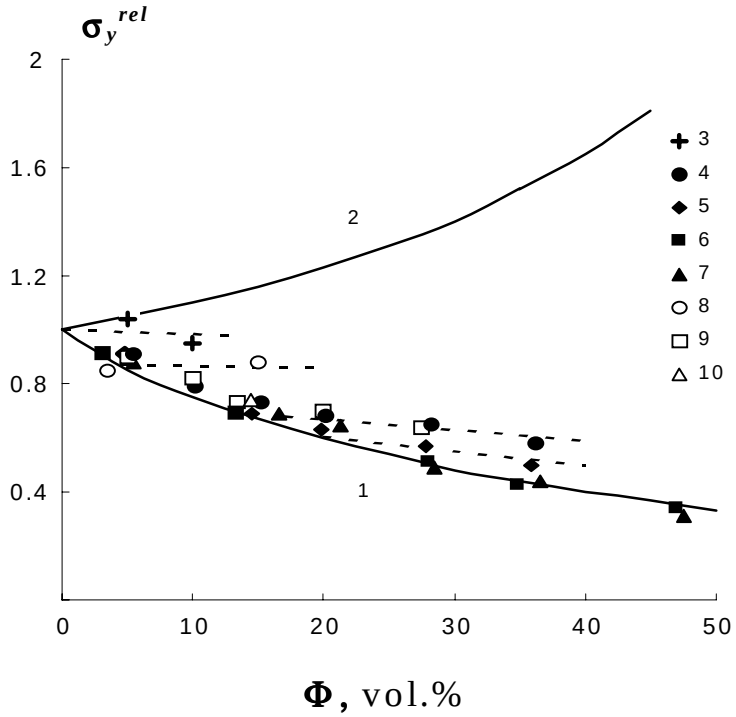

Fig. 2: Composite relative yield stress versus filler fraction, calculated under the assumption of complete debonding (1), perfect interfacial bond (2) and measured for PP (3-7) and HDPE (8-10) based compositions. Mean particles diameter was of 0.2 (3), 1 (4), (8), 2.5 (4), 8 (5), (8), 25 (6), (9) and 55 (7), (10) μm.

$$0 < x_d < 1. \quad (4)$$

The quantitative analysis of the effect of σ_d on $x_d(\Phi)$ and $\sigma_y(\Phi)$ for the uncorrelated and correlated debonding mechanisms was performed. For the polymeric matrices employed, the values of σ_d at identical d are close to each other, and the matrix yield stress, σ_y^m, affects the pattern of the $\sigma_y(\Phi)$ dependencies (Fig. 2).

In the case of

$$\sigma_{d,max} < \sigma_y^m \quad (5)$$

(large inclusions), there is the range of Φ

$$0 < \Phi < \Phi_d \quad (6)$$

where the inequality

$$\sigma_{d,max} < \sigma_{y(d)} \quad (7)$$

is fulfilled and composite yield stress should be described by the basic descending function $\sigma_{y(d)}(\Phi)$. Relation (7) is the condition of the debonding completeness (2) up to the onset of the macroscopic flow. The Φ_d value may be estimated by taking advantage of Eqn 1

$$\Phi_d = \alpha^{-3/2}\left(1-\sigma_{d,max}/\sigma_y^m\right)^{3/2}. \quad (8)$$

It follows from Eqn 8 that the range of filling (6) corresponding to complete debonding becomes narrower with an increase in the debonding stress (i.e., with a decrease in d) and with a decrease in σ_y^m.

Contrary, in the case

$$\sigma_{d,min} > \sigma_y^m \quad (9)$$

(small inclusions), there is a range of Φ

$$0 < \Phi < \Phi_b \quad (10)$$

where the inequality

$$\sigma_{d,min} > \sigma_{y(d)} \quad (11)$$

is fulfilled and composite yield stress should be described by the ascending function $\sigma_{y(b)}(\Phi)$. (11) is the condition of the conservation of the bond during the passage to plastic flow (3). The range (10) becomes narrower with a decrease in σ_d (i.e., with an increase in d) and with an increase in σ_y^m.

At Φ exceeding Φ_d or Φ_b and et every Φ if σ_y^m is inside the range ($\sigma_{d,min}$,$\sigma_{d,max}$) of debonding stresses the interfacial failure appears to be incomplete (4)up to the onset of macroscopic flow. More exactly, the smallest particles remain bonded. The quantitative description of $x_d(\Phi)$ and $\sigma_d(\Phi)$ is reported below.

Uncorrelated debonding

Uncorrelated debonding mechanism anticipates the diffuse distribution of a fraction x of micropores formed to the onset of macroscopic flow by debonding of portion x_d of debonded particles:

$$x = \Phi\, x_d(\Phi) = \Phi\, n(\sigma_y), \quad (12)$$

where $n(\sigma)$ be integral function of debonding stress distribution. This function was approximated in simulations symmetrically by the smooth splines of third order.
The rest portion Φ - x of bonded particles is proposed to be accounted by effective media approach only. Validity of such approximation is supported by the fact that the debonding of large particles is facilitated compared to the case of small ones and thereby large voids are surrounded by matrix with fraction Φ^* of well bonded hard particles of small size. Value of Φ^* is equal to

$$\Phi^* = (\Phi - x)/(1 - x). \quad (13)$$

Yield stress of the effectively uniform matrix can be estimated using calculated in [3] ascending function $\sigma_{y(b)}^{rel}(\Phi)$ (curve 2 of Fig. 2):

$$\sigma_{y(b)}(\Phi^*) = \sigma_y^m \sigma_{y(b)}^{rel}(\Phi^*). \quad (14)$$

Then yield stress of the composite with fraction x of voids and fraction F - x of bonded hard inclusions can be computed using descending function $\sigma_{y(d)}^{rel}(\Phi)$:

$$\sigma_y = \sigma_{y(b)}(\Phi^*)\sigma_{y(d)}^{rel}(x). \quad (15)$$

Substitution of (12) - (14) into relation (15) results in the equation for the composite yield stress:

$$\sigma_y = \sigma_y^m \sigma_{y(b)}^{rel}\left(\Phi \frac{1 - n(\sigma_y)}{1 - \Phi n(\sigma_y)}\right)\sigma_{y(d)}^{rel}\left(\Phi n(\sigma_y)\right). \quad (16)$$

Obviously, Eqn 16 has unique solution σ_y situated between $\sigma_{y(d)}(\Phi)$ and $\sigma_{y(b)}(\Phi)$. This solution in complex with $x_d(\Phi)$ are depicted on Fig. 3a and Fig. 3b correspondingly. It is seen that the proposed model describes the change in the pattern of the concentration dependencies of yield stress (Fig. 2) observed experimentally with varying d. The Φ_d value decreases with an increase in the ratio of debonding to yield stress both due to an increase in σ_d, which may be caused by the drop in particle size, or due a decrease in σ_y^m. The deviation of $\sigma_y(\Phi)$ from basic function $\sigma_{y(d)}(\Phi)$ agrees with a decrease in the fraction of the debonded particles by the onset of the macroscopic flow. The proposed approach allows us to explain the week dependence of the yield stress on Φ for the PP-based composites with d = 0.2 μm (Fig. 2) and the transition from the descending to ascending concentration dependencies observed in [9,11] for ultrafine particles (0.01-0.1 μm).

Correlated debonding

A number of regular trends common with uncorrelated debonding as well as of specific features of the influence of σ_d on $\sigma_y(\Phi)$ and $x_d(\Phi)$ are fulfilled for correlated debonding. Corresponding quantitative analysis is based on an ideal representation of actual process. It is assumed that inside the region of transverse to the loading direction inclusions are debonded, and the microporous zone intersects the entire sample crossection. Thus, it is assumed that the pore volume content x is equal to Φ inside each zone; the overall thickness of craze-like zones per unit length of the sample is equal to x_d.

PP and HDPE filled by high fraction of small particles fail in quasi-brittle manner, i.e. break without previous yielding. Correlated debonding mechanism takes place at high Φ. In view of these facts the analysis is significant only when condition (5) (large particles) is fulfilled.

If the first acts of debonding occur at the stress lower than the calculated value $\sigma_{y(d)}(\Phi)$, that is, when the condition

$$\sigma_{d,min} < \sigma_{y(d)}(\Phi), \tag{17}$$

is fulfilled then in the corresponding filling range

$$0 < \Phi < \Phi_{d(c)} \tag{18}$$

at the moment when the first crazes are formed, the polymer strands separating the pores will be in elastic state and thereby are capable to an increase in the stress. This increase should cause accumulation of craze-like zones, i.e. an increase in x_d. Lift of the load is limited by the value $\sigma_{y(d)}(\Phi)$. Hence concentration dependence of composite yield stress should described by the basic function in the range (18), nevertheless not necessary complete debonding will occur by the onset of macroscopic flow. Similarly to Eqn 8, the $\Phi_{d(c)}$ value may be estimated by taking advantage of Eqn 1 substituting $\sigma_{d,min}$ instead of $\sigma_{d,max}$. Thereby an inequality $\Phi_{d(c)} > \Phi_d$ is fulfilled and contrary to uncorrelated mechanism there exists a filling range

$$\Phi_d < \Phi < \Phi_{d(c)} \tag{19}$$

of not complete debonding, which is also described by basic function.

In the filling range

$$\Phi > \Phi_{d(c)} \tag{20}$$

the condition

$$\sigma_{d,min} > \sigma_{y(d)}(\Phi), \tag{21}$$

is valid. So, just after formation of the primary craze-like zones, the polymer strands are in the state of plastic flow, thus resulting in a drop in the tensile load. In this case the stress-strain curves should have a maximum at the stress $\sigma = \sigma_{d,min}$, which may be considered to be the effective limiting value of the composite yield stress.

This feature of the diagrams is really observed for the materials studied. Because only single inclusions are debonded when $\sigma_{d,min}$ is achieved, x_d and, hence, the number of microporous zones in the filling range (20) should be close to zero. Visual as well as microscopic observation of corresponding samples reveal single deformation zones.

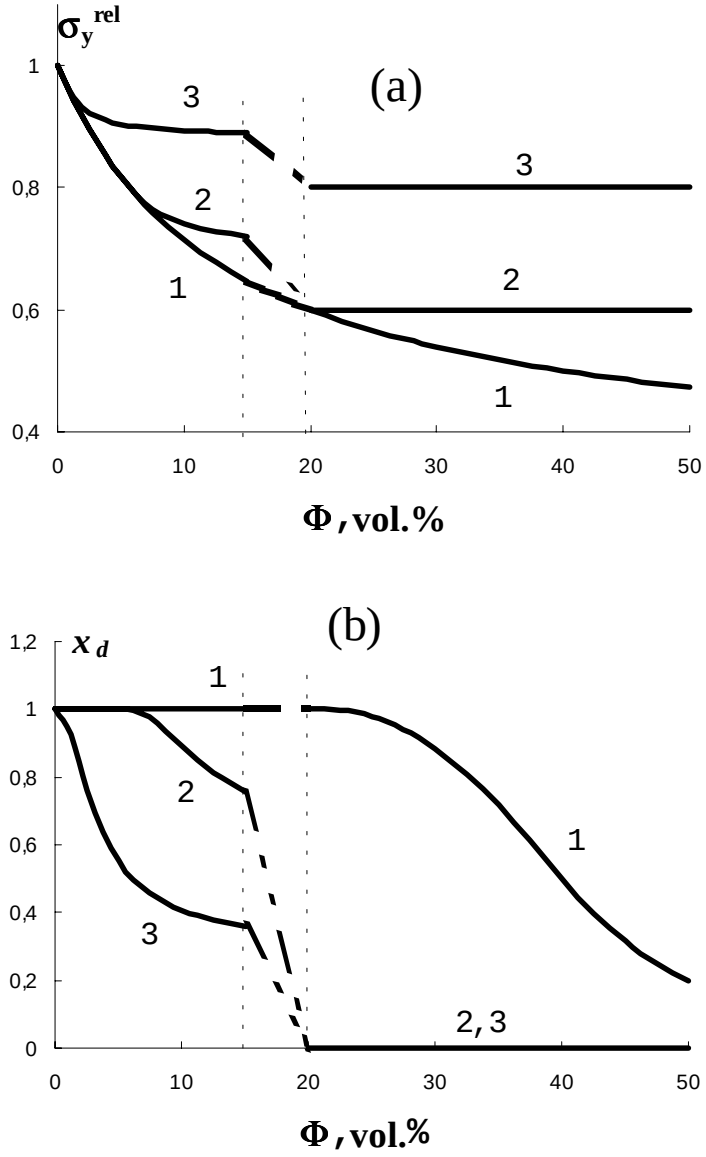

Fig. 3: Concentration dependencies of (a) σ_y^{rel} and (b) x_d calculated at $(\sigma_{d,min},\sigma_{d,max})$= (1) $\left(0{,}4\sigma_y^m, 0{,}6\sigma_y^m\right)$, (2) $\left(0{,}6\sigma_y^m, 0{,}8\sigma_y^m\right)$, and (3) $\left(0{,}8\sigma_y^m, \sigma_y^m\right)$ within the framework of uncorrelated (Φ < 15%) and correlated (Φ > 20%) debonding mechanism.The dashed lines denote the hypothetical transition between the mechanisms.

Fig. 3 represents the $\sigma_y(\Phi)$ (a) and $x_d(\Phi)$ (b) calculated for $\Phi \geq 20\%$ within the framework of correlated debonding mechanism. The curves shown demonstrate the trends discussed. In particular, at low debonding stress (curve 1) filler fraction value corresponded to the deflection from the regime of complete debonding is less than that of the deflection from yield stress basic function.

CONCLUSION

For the high plastic composites with nonideal adhesion, an increase in hard particles fraction results in transition from uncorrelated to correlated debonding mechanism ($\Phi \approx 15$ vol.%) and, correspondingly, in the transition from "uniform" to "craze-like" flow. Concentration dependencies of the composite yield stress are described by the basic descending function corresponded to complete debonding at small Φ, but deflect from the basic curve above critical Φ_d value. The Φ_d value becomes lower with decrease in particle size and/or matrix yield stress. The role of the particle size is explained by the fact that the debonding stress depends on *d*, and thus, in turn, affects the fraction of debonded inclusions. The model proposed describes the effect of the debonding stress on the fraction of the micropores formed by the onset of macroscopic flow and the pattern of the yield stress concentration dependencies. The prediction of the models agree well with experimental data.

REFERENCES

1. Nilsen, L.E., "Mechanical Properties of Polymers and Composites", New York: Marsel Dekker, 1974.

2. Nicolais, L., and Narkis, M., *Polym. Eng. Sci.*, Vol. 11, 1971, p. 1971.

3. Gorbunova, N.V., Knunyants, N.N., Manevitch, L.I., Oshmyan, V.G.,and Topolkaraev, V.A., *Mekh. Kompz. Mater. (Rizh. Poitekh. Inst.),* No. 2, 1990, p. 336.

4. Chacko, V.P., Farris, R.J., and Karasz, F.E., *J. Appl. Polym. Sci.*, Vol. 28, 1983, p. 2701.

5. Dongming, L.I., Wenge, Z., and Zongneng, O.I., *J. Mater. Sci.*, Vol. 29, 1994, p. 3754.

6. Vollenberg, P.H.T., and Heikence, D., *Composite Interfaces. Proc 1 Int. Conf. on Composite Interfaces (ICCI-1),* NewYork: Elsevier, 1986, p. 171.

7. Vollenberg, P.H.T., and Heikence, D., *Polymer,* Vol. 30, No. 9, 1989, p. 1656.

8. Vollenberg, P.H.T., Van de Haan, J.W., Van de Ven, L.J.M., and Heikence, D., *Polymer,* Vol. 30, No. 9, 1989, p. 1663.

9. Sumita, M., Tsukomo, Y., Miyasaka, K., and Jshikawa, K., *J. Mater. Sci.,* Vol. 18, 1983, p. 1757.

10. Pukanszky, B., Fekete, E., and Tudos, F., *Makromol. Chem., Macromol. Symp.,* Vol. 28, 1989, p. 165.

11. Voros, G., and Pukanszky, B., *J. Mater. Sci.,* Vol. 30, 1995, p. 4171.

12. Pukanszky, B., Belina, K., Rockenbauer, A., and Maurer, F.H.J., *Composites,* Vol. 25, No. 3, 1994, p. 205.

13. Muratogly, O.K., Argon, A.S., and Cohen, R.E., *Polymer*, Vol. 36, No. 11, 1995, p. 2143.

14. Gent, A.N., *J. Mater. Sci.*, Vol. 18, 1984, p. 1947.

15. Zhuk, A.V., Knunyants, N.N., Topolkaraev, V.A., Oshmian, V.G., and Berlin, A.A., *J. Mater. Sci.*, Vol. 28, 1993, p. 4595.

16. Fiedrich, K., and Karsch, U.A., *Fiber Sci. Technol.*, Vol. 18, 1983, p. 3752.

17. Wong, F.C., and Ait-Kadi, A., *J. Appl. Polym. Sci.*, Vol. 55, 1995, p. 263.

18. Topolkaraev, V.A., Tovmasyan, Yu.M., Dubnikova, I.L., Petrosyan, A.I., Meshkova, I.N., Berlin, A.A., Gonza, Yu.P., and Shilov, V.V., *Mekh. Kompz. Mater. (Rizh. Poitekh. Inst.)*, No. 4, 1987, p. 616.

19. Dubnikova, I.L., Petrosyan, A.I., Topolkaraev, V.A., Tovmasyan, Yu.M., Meshkova, I.N., and D'yachkovskii, F.S.,. *Vysokomol. Soed.*, Vol. A30, No. 11, 1988, p. 2345.

20. Dubnikova, I.L., Topolkaraev, V.A., Paramzina, T.V., Gorokhova, E.V. and D'yachkovskii, F.S., *Vysokomol. Soed.*, Vol. A32, No. 4, 1990, p. 841.

21. Dubnikova, I.L., Oshmian, V.G., and Gorenberg, A.Ya, *J. Mater. Sci.*, Vol. 32, 1997,
22. p. 1613.

22. Dubnikova, I.L., Muravin, D.K., and Oshmian, V.G., *Polym. Eng. Sci.*, Vol. 37, No. 8, 1997, p. 1301.

23. Muravin, D.K., and Oshmian, V.G., *Comp. Sci. Technol*, Vol. 57, 1997, p. 1167.